



Impact of SM parameters on the spectrum of primordial gravitational waves

Multi-Higgs Models 2022

João Viana

with F.Freitas, G.Lourenço, A.Morais, A. Nunes, J. Olívia, R. Pasechnik, R. Santos

Impact of SM parameters and of the vacua of the Higgs potential in gravitational waves detection
(arXiv:2108.12810 - JCAP 03 (2022) 046)

Tuesday, 30th August 2022

Motivation

The **SM** lacks an out of equilibrium epoch, a condition for **baryogenesis** (Sakharov (1967))

We propose an extended model

SM + Complex Scalar Field

This model allows for an **first order electroweak phase transition (EWPT)**.

A possible way to detect such transition is by measuring the **primordial gravitational waves** spectrum created by sound waves.

We explored the parameter space and tested the **GW spectrum** dependence on the SM parameters.

This model also produces a dark matter candidate, a missing piece of the **SM**.

Scalar Potential

We add a complex scalar field ($Y_\sigma = T_\sigma = 0$) to the Standard Model content and choose the potential

$$\mathcal{V}_0(\Phi, \sigma) = \underbrace{\mu_\Phi^2 \Phi^\dagger \Phi + \lambda_\Phi (\Phi^\dagger \Phi)^2}_{\text{Standard Model}} + \mu_\sigma^2 \sigma^* \sigma + \lambda_\sigma (\sigma^* \sigma)^2 + \lambda_{\Phi\sigma} \Phi^\dagger \Phi \sigma^* \sigma + \left(\frac{1}{2} \mu_b^2 \sigma^2 + \text{h.c.} \right),$$

where

$$\Phi = \frac{1}{\sqrt{2}} \begin{pmatrix} G + iG' \\ \phi_h + h + i\eta \end{pmatrix}, \quad \sigma = \frac{1}{\sqrt{2}} (\phi_\sigma + \sigma_R + i\sigma_I).$$

We enforce the \mathbb{Z}_2 symmetry $\sigma \rightarrow -\sigma$ making all potential parameters real. The vacuum configuration is

$$\langle \Phi \rangle = \frac{1}{\sqrt{2}} \begin{pmatrix} 0 \\ \phi_h \end{pmatrix} \stackrel{T=0}{=} \frac{1}{\sqrt{2}} \begin{pmatrix} 0 \\ v_h \end{pmatrix}, \quad \langle \sigma \rangle = \frac{1}{\sqrt{2}} \phi_\sigma \stackrel{T=0}{=} \frac{1}{\sqrt{2}} v_\sigma.$$

Scenarios

Scenario 1 ($v_\sigma \neq 0$)

- 2 Real Scalar Particles (1 Higgs-like)
- 1 Dark Matter Particle

Scenario 2 ($v_\sigma \neq 0 + \text{neutrinos}$)

- 2 Real Scalar Particles (1 Higgs-like)
- 1 Dark Matter Particle
- 6 Majorana Sterile Neutrinos

Finite Temperature Potential

The 1-loop finite temperature potential is given by

$$V_{\text{eff}}(T) = V_0 + V_{\text{CW}}^{(1)} + V_{\text{ct}} + \Delta V(T),$$

where V_0 is the tree-level classical scalar potential.

The zero temperature 1-loop Coleman-Weinberg (CW) potential is given by

$$V_{\text{CW}} = \sum_i (-1)^{F_i} n_i \frac{m_i^4(\phi_\alpha)}{64\pi^2} \left(\log \left[\frac{m_i^2(\phi_\alpha)}{\Lambda^2} \right] - c_i \right),$$

where $F_i = 0(1)$ for bosons(fermions), m_i are the ϕ_α field-dependent masses, n_i are the number of d.o.f. for particle i , Λ is the $\overline{\text{MS}}$ renormalization constants, and c_i are $\frac{3}{2}$ for each d.o.f. of scalars, fermions and longitudinally polarised gauge bosons and $\frac{1}{2}$ for each d.o.f. of transversely polarised gauge boson, in the Landau gauge.

Finite Temperature Potential - Counterterms and Temperature Corrections

The counterterm potential is given by

$$V_{\text{ct}} = \delta\mu_\Phi^2 \Phi^\dagger \Phi + \delta\lambda_\Phi (\Phi^\dagger \Phi)^2 + \delta\mu_\sigma^2 \sigma^* \sigma + \delta\lambda_\sigma (\sigma^* \sigma)^2 \\ + \delta\lambda_{\Phi\sigma} \Phi^\dagger \Phi \sigma^* \sigma + \left(\frac{1}{2} \delta\mu_b^2 \sigma^2 + \text{h.c.} \right).$$

We apply the renormalization conditions by imposing that tadpole equations and mass terms are unchanged at 1-loop

$$\left\langle \frac{\partial V_{\text{ct}}}{\partial h_i} \right\rangle = \left\langle -\frac{\partial V_{\text{CW}}^{(1)}}{\partial h_i} \right\rangle, \quad \left\langle \frac{\partial^2 V_{\text{ct}}}{\partial h_i \partial h_j} \right\rangle = \left\langle -\frac{\partial^2 V_{\text{CW}}^{(1)}}{\partial h_i \partial h_j} \right\rangle.$$

The 1-loop finite-temperature corrections are given by (Quiros (1999))

$$\Delta V(T) = \frac{T^4}{2\pi^2} \left\{ \sum_b n_b J_B \left[\frac{m_i^2(\phi_\alpha)}{T^2} \right] - \sum_f n_f J_F \left[\frac{m_i^2(\phi_\alpha)}{T^2} \right] \right\},$$

where n_b (n_f) are the bosonic (fermionic) d.o.f. for each particle b (f) in the summation, and m_i are the field dependent masses. The $J_{B/F}$ functions are the bosonic (fermionic) thermal integrals given by

$$J_{B/F}(y^2) = \int_0^\infty dx x^2 \log \left(1 \mp \exp \left[-\sqrt{x^2 + y^2} \right] \right).$$

Finite Temperature Potential - Temperature Corrections

At finite temperature one also has to take into account the daisy (ring) diagrams to compute consistently at a given order (Arnold and Espinosa (1993), Dolan and Jackiw (1974), Espinosa and Quiros (1995), Parwani (1992)).

This is done by resumming higher-loop diagrams which, in practice, is equivalent to have a temperature-dependent mass term

$$\mu_\alpha^2(T) = \mu_\alpha^2 + c_\sigma T^2.$$

In scenario 2, the daisy correction c_σ receives an additional contribution coming from the neutrino Yukawa sector of the form

$$c_\sigma \rightarrow c_\sigma + \frac{1}{24} \sum_{i=1}^3 Y_{\sigma i}^2,$$

The longitudinal modes of the gauge bosons also receives thermal corrections

$$m_{W_L}^2(\phi_h; T) = m_W^2(\phi_h) + \frac{11}{6} g^2 T^2,$$

$$m_{Z_L, A_L}^2(\phi_h; T) = \frac{1}{2} m_Z^2(\phi_h) + \frac{11}{12} (g^2 + g'^2) T^2 \pm \mathcal{D},$$

where

$$\mathcal{D}^2 = \left(\frac{1}{2} m_Z^2(\phi_h) + \frac{11}{12} (g^2 + g'^2) T^2 \right)^2 - \frac{11}{12} g^2 g'^2 T^2 \left(\phi_h^2 + \frac{11}{3} T^2 \right).$$

Instanton

The decay rate of the false vacuum to the true vacuum is given (Coleman (1977)) by

$$\Gamma(T) = A(T) e^{-\hat{S}_3/T},$$

where \hat{S}_3/T is the O(3) symmetric Euclidian action given by

$$\hat{S}_3(\hat{\phi}, T) = 4\pi \int_0^\infty dr r^2 \left\{ \frac{1}{2} \left(\frac{d\hat{\phi}}{dr} \right)^2 + V_{\text{eff}}(\hat{\phi}, T) \right\},$$

with $\hat{\phi}$ being the field VEVs that follow the classical path

$$\frac{d^2\hat{\phi}}{dr^2} + \frac{2}{r} \frac{d\hat{\phi}}{dr} = \frac{dV_{\text{eff}}}{d\hat{\phi}}, \text{ with boundary conditions } \hat{\phi}(r)|_{r \rightarrow \infty} = 0, \quad \frac{d\hat{\phi}}{dr}|_{r=0} = 0.$$

The prefactor $A(T)$ of the tunnelling rate can be well approximated as

$$A(T) \simeq T^4 \left(\frac{\hat{S}_3}{2\pi T} \right)^{\frac{3}{2}}$$

Temperatures

- ▶ **Critical Temperature - T_c** - The potential has two degenerate minima and, consequently, the transition from the false vacuum to the true vacuum begins via quantum tunnelling.
- ▶ **Nucleation Temperature - T_n** - The temperature at which the tunnelling decay rate matches the Hubble rate

$$\frac{\Gamma(T_n)}{H^4(T_n)} = 1 .$$

- ▶ **Percolation Temperature - T_*** - Temperature at which at least 34% of the false vacuum has tunnelled into the true vacuum or, equivalently, the probability of finding a point still in the false vacuum is 70%

$$P(T) = e^{-I(T)}, \quad I(T) = \frac{4\pi v_b^3}{3} \int_T^{T_c} \frac{\Gamma(T')dT'}{T'^4 H(T')} \left(\int_T^{T'} \frac{d\tilde{T}}{H(\tilde{T})} \right)^3$$

To find the percolation temperature one has to solve $I(T_*) = 0.34$ or, equivalently, $P(T_*) = 0.7$.

There is a clear hierarchy between the temperatures

$$T_c > T_n > T_*$$

Strength of the Phase Transitions

The strength of the phase transitions is defined by the trace anomaly Hindmarsh et al. (2015, 2017) as

$$\alpha = \frac{1}{\rho_\gamma} \left[V_i - V_f - \frac{T_*}{4} \left(\frac{\partial V_i}{\partial T} - \frac{\partial V_f}{\partial T} \right) \right].$$

The inverse time scale of the transitions if given by

$$\frac{\beta}{H} = T_* \left. \frac{d}{dT} \left(\frac{\hat{S}_3(T)}{T} \right) \right|_{T_*}.$$

The order parameter of the phase transition is given by

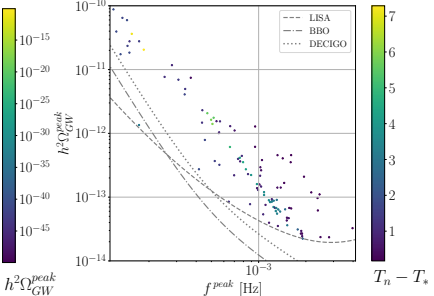
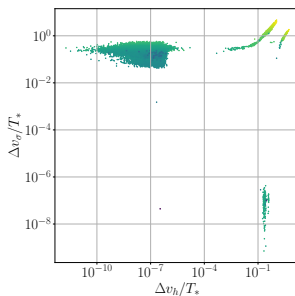
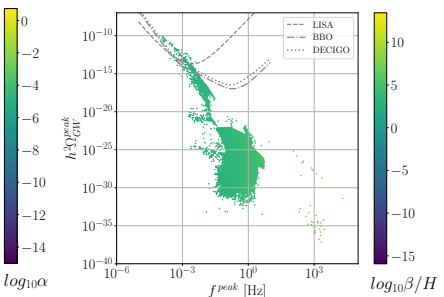
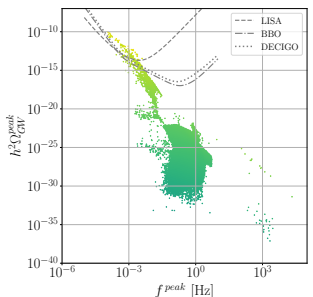
$$\frac{\Delta v_\phi}{T_*} = \frac{|v_\phi^f - v_\phi^i|}{T_*}, \quad \phi = h, \sigma.$$

The spectrum of the GW is given by

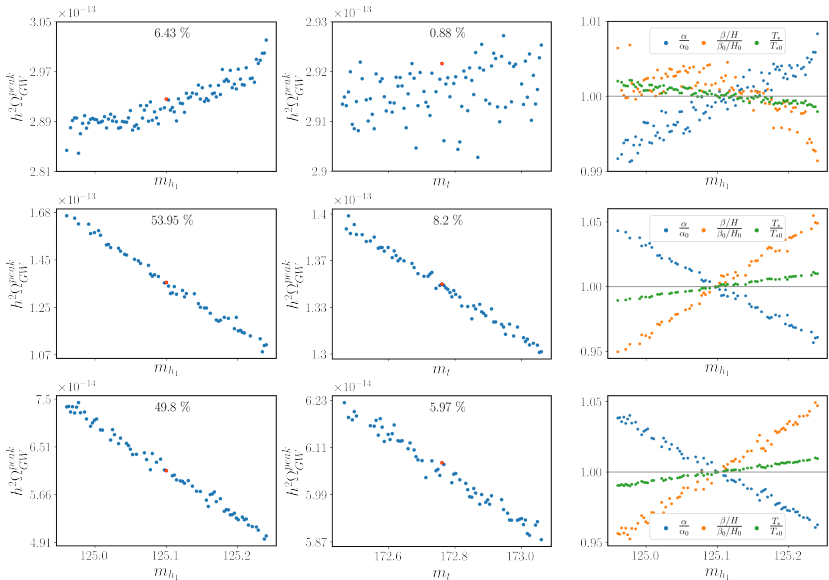
$$h^2 \Omega_{\text{GW}} = h^2 \Omega_{\text{GW}}^{\text{peak}} \left(\frac{4}{7} \right)^{-\frac{7}{2}} \left(\frac{f}{f_{\text{peak}}} \right)^3 \left[1 + \frac{3}{4} \left(\frac{f}{f_{\text{peak}}} \right) \right]^{-\frac{7}{2}},$$

where f_{peak} is proportional to the inverse of the mean bubble separation.

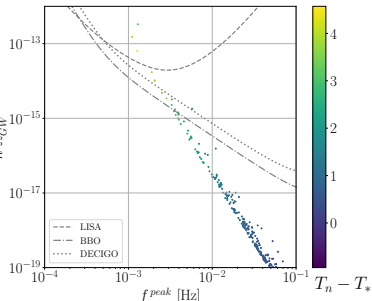
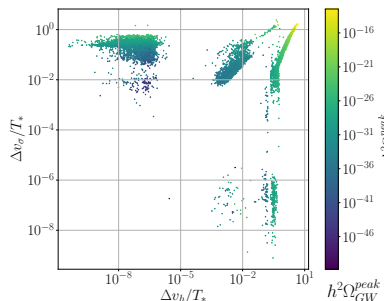
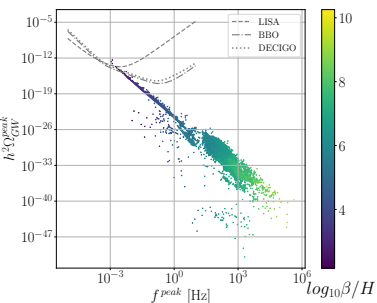
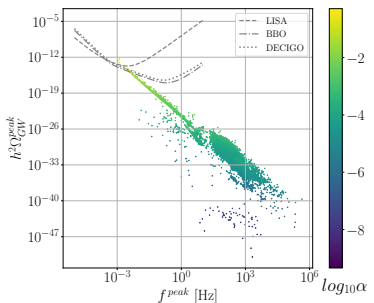
Scenario 1 - Results



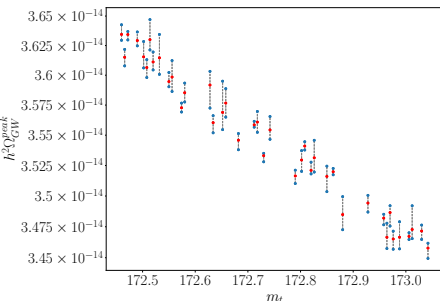
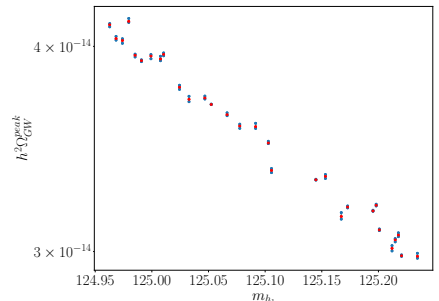
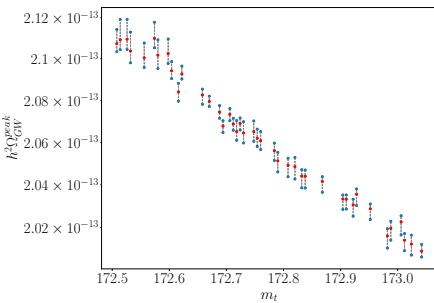
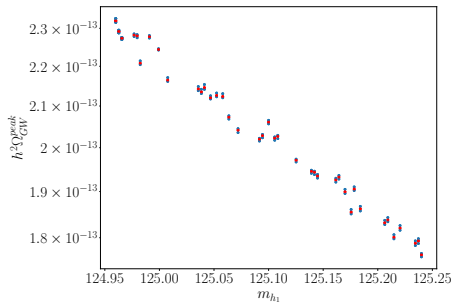
Scenario 1 - Variations with Higgs and Top Quark Mass



Scenario 2 - Results



Scenario 2 - Variations with Higgs and Top Quark Mass



Conclusions

- Detectable GW occur when both order parameters fulfill $\frac{\Delta v_\phi}{T_*} \sim 1$.
- Strong transitions have a significant difference in percolation and nucleation temperatures.
- In scenario 1, at most **250%** GW signal variation if we vary the Higgs mass inside its experimental uncertainty.
- In scenario 1, at most **12%** GW signal variation if we vary the top mass.
- In scenario 2, at most **25%** GW signal variation if we vary the Higgs mass.
- In scenario 2, at most **5%** GW signal variation if we vary the top mass.
- There is no impact if we vary the any other SM parameter inside its experimental uncertainty.
- Weak points, with $\frac{\Delta v_\phi}{T_*} \ll 1$, do not have any variation with any SM parameter (including Higgs/Top mass).

Peter Brockway Arnold and Olivier Espinosa. The Effective potential and first order phase transitions: Beyond leading-order. *Phys. Rev. D*, 47:3546, 1993. doi: 10.1103/PhysRevD.47.3546. [Erratum: Phys.Rev.D 50, 6662 (1994)].

Chiara Caprini et al. Detecting gravitational waves from cosmological phase transitions with LISA: an update. *JCAP*, 2003(03):024, 2020. doi: 10.1088/1475-7516/2020/03/024.

Sidney R. Coleman. The Fate of the False Vacuum. 1. Semiclassical Theory. *Phys. Rev.*, D15:2929–2936, 1977. doi: 10.1103/PhysRevD.15.2929,10.1103/PhysRevD.16.1248. [Erratum: Phys. Rev.D16,1248(1977)].

L. Dolan and R. Jackiw. Symmetry Behavior at Finite Temperature. *Phys. Rev.*, D9:3320–3341, 1974. doi: 10.1103/PhysRevD.9.3320.

J. R. Espinosa and M. Quiros. Improved metastability bounds on the standard model Higgs mass. *Phys. Lett. B*, 353:257–266, 1995. doi: 10.1016/0370-2693(95)00572-3.

Mark Hindmarsh, Stephan J. Huber, Kari Rummukainen, and David J. Weir. Numerical simulations of acoustically generated gravitational waves at a first order phase transition. *Phys. Rev.*, D92(12):123009, 2015. doi: 10.1103/PhysRevD.92.123009.

Mark Hindmarsh, Stephan J. Huber, Kari Rummukainen, and David J. Weir. Shape of the acoustic gravitational wave power spectrum from a first order phase transition. *Phys. Rev. D*, 96(10):103520, 2017. doi: 10.1103/PhysRevD.96.103520. [Erratum: Phys.Rev.D 101, 089902 (2020)].

Rajesh R. Parwani. Resummation in a hot scalar field theory. *Phys. Rev. D*, 45:4695, 1992. doi: 10.1103/PhysRevD.45.4695. [Erratum: Phys.Rev.D 48, 5965 (1993)].

Mariano Quiros. Finite temperature field theory and phase transitions. In *ICTP Summer School in High-Energy Physics and Cosmology*, 1 1999.

A. D. Sakharov. Violation of CP Invariance, C asymmetry, and baryon asymmetry of the universe. *Pisma Zh. Eksp. Teor. Fiz.*, 5:32–35, 1967. doi: 10.1070/PU1991v034n05ABEH002497.

Carroll L. Wainwright. Cosmotransitions: Computing cosmological phase transition temperatures and bubble profiles with multiple fields. *Computer Physics Communications*, 183(9):20062013, Sep 2012. ISSN 0010-4655. doi: 10.1016/j.cpc.2012.04.004. URL <http://dx.doi.org/10.1016/j.cpc.2012.04.004>.

Thank you!

Questions?

Scenario 2 - Neutrino Potential

In scenario 2 we considered an inverse-seesaw mechanism given by

$$\mathcal{L}_{\text{CxSM}} = (\dots) - Y_h \overline{L_\beta} \tilde{\Phi} N_R - M_\nu \overline{S_R^c} N_R - \frac{1}{2} \tilde{\mu} \overline{S_R^c} S_R \sigma + \text{h.c.} .$$

It has the following mass matrix, with $m_D \equiv Y_h \frac{v_h}{\sqrt{2}}$, $\mu \equiv \tilde{\mu} \frac{v_\sigma}{\sqrt{2}}$,

$$\mathcal{L}_{\text{CxSM}}^{\text{bilinear}} = (\dots) - \frac{1}{2} \begin{pmatrix} \overline{v_L} & \overline{N_R^c} & \overline{S_R^c} \end{pmatrix} \begin{pmatrix} 0 & m_D & 0 \\ m_D & 0 & M_\nu \\ 0 & M_\nu & \mu \end{pmatrix} \begin{pmatrix} v_L^c \\ N_R \\ S_R \end{pmatrix} + \text{h.c.} .$$

We impose the following hierarchy $M_\nu \gg m_D \gg \mu$ which enables us to approximate light left handed neutrino (SM-like) mass as

$$m_{\nu_1} \approx \mu \frac{m_D^2}{M_\nu^2} ,$$

We also have two Majorana neutrinos, with large masses, approximately equal to

$$\begin{aligned} m_{\nu_2} &\approx M_\nu + \frac{m_D}{2} , \\ m_{\nu_3} &\approx M_\nu - \frac{m_D}{2} . \end{aligned}$$

Gravitational Waves Spectrum

The spectrum of the GW is given by

$$h^2 \Omega_{\text{GW}} = h^2 \Omega_{\text{GW}}^{\text{peak}} \left(\frac{4}{7} \right)^{-\frac{7}{2}} \left(\frac{f}{f_{\text{peak}}} \right)^3 \left[1 + \frac{3}{4} \left(\frac{f}{f_{\text{peak}}} \right) \right]^{-\frac{7}{2}},$$

where f_{peak} is the peak-frequency. Semi-analytic expressions for peak-amplitude and peak-frequency in terms of β/H and α can be found in Ref. (Caprini et al. (2020)) and can be written as

$$f_{\text{peak}} = 26 \times 10^{-6} \left(\frac{1}{HR} \right) \left(\frac{T_*}{100} \right) \left(\frac{g_*}{100 \text{ GeV}} \right)^{\frac{1}{6}} \text{ Hz},$$

$$h^2 \Omega_{\text{GW}}^{\text{peak}} = 1.159 \times 10^{-7} \left(\frac{100}{g_*} \right) \left(\frac{HR}{\sqrt{c_s}} \right)^2 K^{\frac{3}{2}}, \text{ for } H\tau_{\text{sh}} = \frac{2}{\sqrt{3}} \frac{HR}{K^{1/2}} < 1,$$

$$h^2 \Omega_{\text{GW}}^{\text{peak}} = 1.159 \times 10^{-7} \left(\frac{100}{g_*} \right) \left(\frac{HR}{c_s} \right)^2 K^2, \text{ for } H\tau_{\text{sh}} = \frac{2}{\sqrt{3}} \frac{HR}{K^{1/2}} \simeq 1,$$

Gravitational Waves

The fraction of the kinetic energy in the fluid compared the total bubble energy is given by

$$K = \frac{\kappa\alpha}{1+\alpha},$$

and

$$HR = \frac{H}{\beta} (8\pi)^{\frac{1}{3}} \max(v_b, c_s),$$

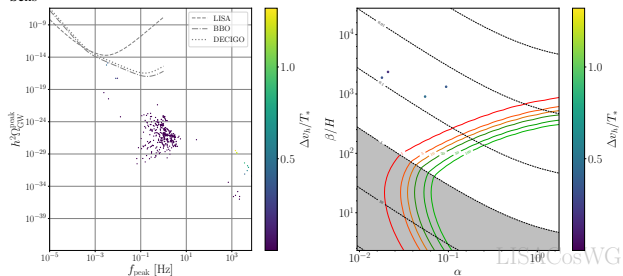
where κ is the efficiency factor. The bubble wall velocity has to be large enough to give rise to detectable GWs spectra. Our analysis is performed using `CosmoTransitions` (Wainwright (2012)), considering the case of supersonic detonations where the wall velocity $v_b = 0.95$ is taken to be above the Chapman-Jouguet limit,

$$v_J = \frac{1}{1+\alpha} \left(c_s + \sqrt{\alpha^2 + \frac{2}{3}\alpha} \right).$$

Signal-to-noise Ratio - Scenario 1 vs Scenario 2

$$\text{SNR} = \sqrt{\mathcal{T} \int_{f_{\min}}^{f_{\max}} df \left[\frac{h^2 \Omega_{\text{GW}}(f)}{h^2 \Omega_{\text{Sens}}(f)} \right]^2}$$

$v_\sigma \neq 0$



$v_\sigma \neq 0 + \text{neutrinos}$

